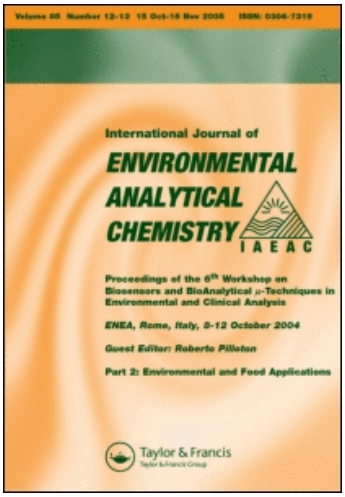

International Journal of Environmental Analytical Chemistry

Publication details, including instructions for authors and subscription information:
http://www.informaworld.com/smpp/title~content=t713640455

Complexation of gadolinium(III) ions on top of nanometre-sized magnetoliposomes

Stefaan J. H. Soenen[a]; Linda Desender[a]; Marcel De Cuyper[a]
[a] Interdisciplinary Research Center, Katholieke Universiteit Leuven—Campus Kortrijk, B-8500 Kortrijk, Belgium

Online publication date: 18 November 2010

To cite this Article Soenen, Stefaan J. H. , Desender, Linda and Cuyper, Marcel De(2007) 'Complexation of gadolinium(III) ions on top of nanometre-sized magnetoliposomes', International Journal of Environmental Analytical Chemistry, 87: 10, 783 — 796

To link to this Article: DOI: 10.1080/03067310701336320

URL: http://dx.doi.org/10.1080/03067310701336320

Intern. J. Environ. Anal. Chem.
Vol. 87, Nos. 10–11, 20 August–15 September 2007, 783–796

Complexation of gadolinium(III) ions on top of nanometre-sized magnetoliposomes

STEFAAN J. H. SOENEN, LINDA DESENDER and MARCEL DE CUYPER*

Interdisciplinary Research Center, Katholieke Universiteit Leuven—Campus Kortrijk, University Campus, B-8500 Kortrijk, Belgium

(*Received 16 September 2006; in final form 10 March 2007*)

The complex of diethylenetriaminepentaacetate (DTPA) with the paramagnetic gadolinium ion [Gd(III)] is a well-known blood pool contrast agent for magnetic resonance imaging (MRI). To obtain MRI pictures from other anatomical structures, for instance from tissues containing cells with phagocytic activity, larger colloidal complexes have to be constructed. Therefore, in view of modifying the physiological behaviour, the DTPA chelate was first hydrophobized by covalently linking it to phosphatidylethanolamine (PE), and the resulting conjugate was then incorporated into nanometre-sized, sonicated phospholipid vesicles. Qualitative information on the affinity of the PE–DTPA derivative for Gd(III) ions was derived from competition experiments using the dye Arsenazo. Furthermore, it was found that only the membranotropic adducts residing in the outer shell of the vesicle bilayer are accessible to the lanthanide ion. The vesicular particulate was also used as a vehicle to transport PE–DTPA into the coating of so-called magnetoliposomes which consist of nanometre-sized iron oxide cores onto which a phospholipid bilayer is strongly chemisorbed. After loading the resulting structures with Gd(III), this new type of magnetoliposome may offer unique potentialities as a novel *bi*-label MRI contrast medium.

Keywords: Diethylenetriaminepentaacetate (DTPA); Gadolinium; Liposome; Magnetoliposome; MRI contrast agent; Phospholipid vesicle

1. Introduction

The concern about the toxicity of heavy metals takes a central position in many studies dealing with the relationship between environment and health. Although the mechanisms for the toxic actions are not fully understood, in general terms blocking of essential enzymes, receptors, cellular functions, etc. have been reported [1–5]. In view of the toxic effects, at first sight, it may be very surprising that heavy metal ions are purposely used in selected medical *in vivo* applications. For instance, to improve the conspicuousness of lesions, the visualization of blood vessels or, in general, the diagnosis of numerous types of illnesses, gadolinium often acts as the key element in conventional magnetic resonance imaging (MRI) contrast agents. Although the

*Corresponding author. Fax: +32-56-246997. Email: marcel.decuyper@kuleuven-kortrijk.be

International Journal of Environmental and Analytical Chemistry
ISSN 0306-7319 print/ISSN 1029-0397 online © 2007 Taylor & Francis
DOI: 10.1080/03067310701336320

transition-metal ion itself is not visible in MRI, only the impact of the paramagnetic features (gadolinium has seven unpaired electrons in the 4f valence shell) on (mainly) hydrogen nuclei located in the immediate vicinity of gadolinium is monitored. In MRI, indeed, the magnetic moments of the protons, which are oriented randomly, are first aligned in an externally applied magnetic field. Upon transmission of an appropriate radiofrequency pulse, this directed orientation is perturbed, and the time needed for recovery to the original aligned state (the so-called spin-lattice relaxation time T_1) is exploited to create a (positive) signal. As a consequence, image contrast results from differences in water densities and in T_1 relaxation times between adjacent tissues, or at tissue–blood boundaries. The presence of paramagnetic ions, if located in close proximity to hydrogen nuclei, will further drastically reduce the T_1 value and may further improve the contrast (see [6–10] for more information on the basics of MRI).

At the levels used for MRI, however, Gd(III) is too toxic, and consequently it cannot be injected as such. To ensure its innocuousness during its route through the body, the free ion has to be captured in the claw of chelating organic molecules such as diethylenetriaminepentaacetate (DTPA) (figure 1a). Within the DTPA–Gd(III) polydentate complex, the lanthanide ion has nine coordination sites: it is linked to

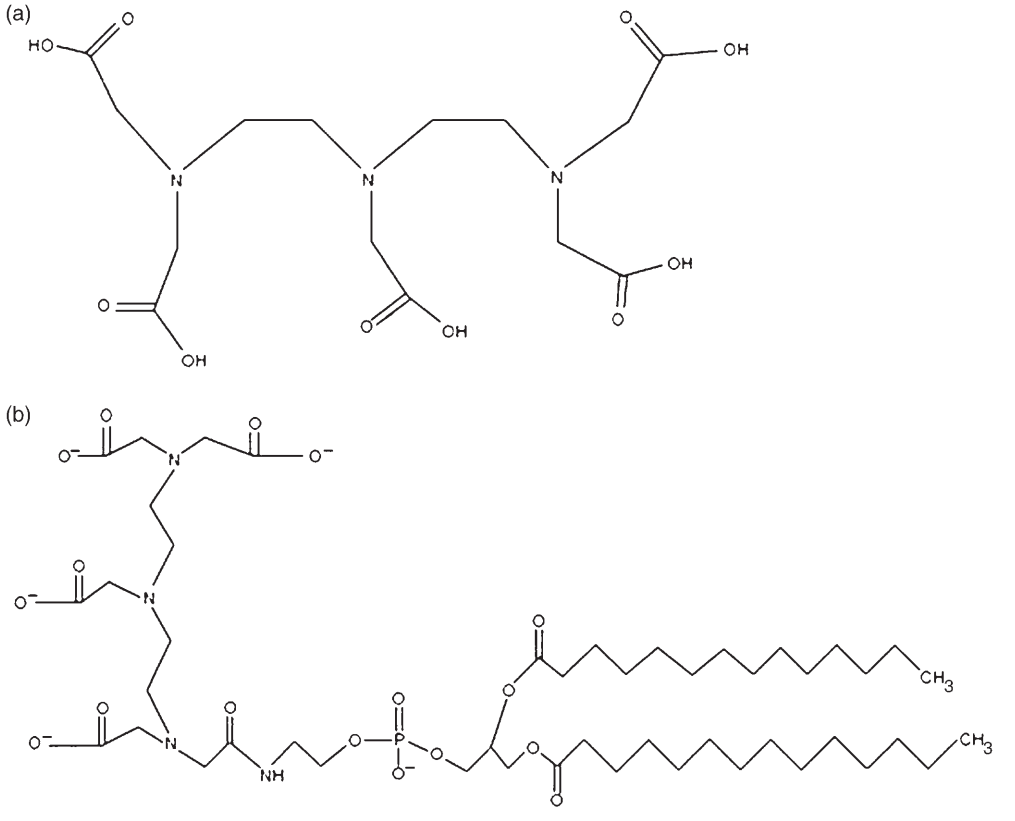

Figure 1. Structural formulae of the Gd-chelators (a) diethylenetriaminepentaacetate (DTPA) and (b) 1,2-dimyristoyl-*sn*-glycero-3-phosphoethanolaminediethyletriaminepentaacetate (DMPE–DTPA).

the three nitrogen atoms and to the five –COOH groups. At the vacant ninth site, it can bind a single water molecule, rendering the complex a highly effective relaxation agent [11, 12].

In clinical applications, the Gd(III)–DTPA complex is frequently used for angiographic purposes, but a main weakness of this low-molecular-weight contrast agent is its relatively fast blood clearance via the urinary tract [13]. On the other hand, macromolecular structures in which DTPA–Gd(III) is linked to albumin, dextran, polylysin, dendrimers, or micelles are expected to have a longer blood residence, and thus data acquisition can occur over a longer time window, ultimately resulting in enhanced sensitivity [14–18]. An additional advantage of immobilizing DTPA–Gd(III) complexes on polymers is that the contrast generated by each individual complex considerably improves as a result of a reduction in tumbling rate of the entire supramolecular structure [8, 12].

In the present work, we elaborate on the issue of supramolecular contrast agents by covering the surface of nanometre-sized liposomal structures with a layer of Gd(III) ions. To this end, the complexing DTPA moieties were first conjugated covalently, via one of its –COOH functional groups, to the $-NH_2$ present in the polar part of phosphatidylethanolamine (PE). Since the resulting PE–DTPA adduct is not soluble in aqueous medium, it is first assembled in phospholipid vesicles or liposomes which act as carriers, and then the ability of these colloidal particles to bind Gd(III) ions is tested. Alternatively, the PE–DTPA membranotropic amphiphile is also incorporated into the coating layer of so-called magnetoliposomes (MLs), consisting of nanometre-sized iron oxide cores covered by a phospholipid bilayer and then loaded with Gd(III) ions. We briefly outline the potential of this special type of ML, which combines Gd and magnetite (Fe_3O_4), as a new-generation MRI contrast medium on the horizon. The use of this novel double label contrast agent, indeed, may allow the radiologist to gather T_1 and T_2^* weighted images with improved contrast.

2. Experimental

2.1 *Materials*

N-Tris[hydroxymethyl]methyl-2-aminoethanesulfonic acid (TES), $GdCl_3 \cdot 6aq$, triethylamine, and DTPA were supplied by Sigma-Aldrich Chemie GmbH (Deisenhofen, Germany). The bicyclic anhydride form of DTPA was a Dojindo Laboratories product (SopaChem, Eke, Belgium). Arsenazo III (2,2′-[1,8-dihydroxy-3,6-disulfonaphthylene-2,7-bisazo]-bisbenzene arsonic acid) was purchased from Merck-Eurolab (Darmstadt, Germany). The phospholipids, 1,2-dimyristoyl-*sn*-glycero-3-phosphocholine (DMPC), 1,2-dimyristoyl-*sn*-glycero-3-(phospho-1-glycerol) (DMPG), and 1,2-dimyristoyl-*sn*-glycero-3-phosphoethanolamine (DMPE) were obtained from Avanti Polar Lipids (Alabaster, AL). All solvents and chemicals used for TLC were of analytical grade and were purchased from Sigma-Aldrich or Merck-Eurolab. The organic solvents (SeccoSolv grade) used in synthesis protocols were further dehydrated by adding Molecular Sieves 0.4 nm (Merck-Eurolab).

Synthesis of the DTPA–phosphatidylethanolamine derivative (PE–DTPA) (figure 1b) abides by a modified version of the approach described by Torchilin *et al*. [19] and proceeds as follows: to 111.9 μmol DTPA anhydride dissolved in 2 mL of dioxane,

13.36 μmol of PE solubilized in 0.4 mL of chloroform containing 0.3 μmol triethylamine was added dropwise over 3 min while shaking vigorously. (As opposed to the procedure described by Torchilin *et al*. [19], dioxane was used instead of DMSO, since the latter produced a weird yellow haze covering the upper part of the TLC plate, thereby hampering clear identification of the spots.) Note that, to avoid formation of a dimeric byproduct in which two PEs are linked to one DTPA residue [20], an 8.4-fold molar excess of DTPA *bis*-anhydride (or a 16.8-fold equivalent excess of reactive anhydride groups) to phospholipid is used. The reaction proceeds for 3 h at room temperature while being stirred continuously. Reaction progress was verified by analytical TLC (Silicagel 60 aluminium sheets, 0.2 mm layer thickness; Merck-Eurolab) using a chloroform/methanol/water mixture (65/25/4; v/v) as eluting solvent. The parent PE molecule was used as reference. Two separate plates were spotted in the same way and eluted in identical experimental conditions (not shown). After thoroughly drying the plates, one was treated with ninhydrin (0.5 g solubilized in 50 mL of chloroform) which enables detection of free amino groups. The second plate was sprayed with phosphomolybdenium reagent to visualize the presence of phosphate [21]. In the lanes of both the pure PE reference and the reaction mixture, only one positive amino spot with an R_f of 0.8 was found. On the second plate, stained for phosphate, two spots with R_f values of 0.2 and 0.8 were detected for the reaction mixture, whereas in the PE lane, only the R_f 0.8 spot was visible. This indicates that the $-NH_2$ group in the phospholipid eluting with an $R_f = 0.2$ is blocked by the DTPA moiety. Phosphate analysis of both spots of the reaction mixture revealed a reaction efficiency of about 50%. Isolation of the desired PE–DTPA adduct on a preparative scale is done on preparative glass coated Silicagel 60 (1 mm layer thickness with concentration zone) TLC plates (Merck-Eurolab) using the same elution solvent system. The conjugate was stored in a lyophilized form. The protocol described above was successfully used to prepare PE–DTPA derivatives bearing various types of fatty acyl chains. In the present work, only the dimyristoyl analogue (DMPE–DTPA) is used.

2.2 *Methods*

2.2.1 Vesicle formation. To prepare the vesicles, the chloroform solvent used to solubilize the phospholipid(s) was removed by evaporation, and the dried film was hydrated to the desired lipid density using a 5 mM TES buffer, pH 7.0. The resulting suspension was then sonicated using a probe tip sonicator (MSE 150 W Ultrasonic Desintegrator) at an amplitude between 18 and 24 μ peak-to-peak using a 3/8-inch probe in a jacked vessel, which was made to our specifications and allowed continuous temperature control. During sonication, the temperature was kept at 25°C, which is slightly above the gel-to-liquid crystal phase transition temperature of the phospholipids (T_m DMPC and T_m DMPG ≈ 23°C). Initially, a milky suspension was formed, which, upon further sonication for 10 min, gradually turned to a clear solution of small unilamellar vesicles. To remove titanium dust released from the sonication tip, the solution was centrifuged for 10 min at 5000 *g*.

2.2.2 Magnetoliposome formation. Magnetoliposomes were produced by a method developed in our lab [22]. In brief, we start from magnetite (Fe_3O_4) cores coated with

lauric acid, which were synthesized by chemical co-precipitation from an aqueous solution of Fe(II) and Fe(III) salts with ammonia. The detailed procedure to prepare this water-adapted magnetic fluid can be found in [23]. To generate magnetite–phospholipid complexes (so-called MLs), surfactant-stabilized magnetic nanoparticles and phospholipid vesicles were mixed (mmol phospholipid/g magnetite = 5) and then exhaustively dialysed (Spectra/Por® No2 dialysis membrane tubing, molecular weight cutoff 12,000–14,000; Spectrum Europe, Breda, The Netherlands) for 3 days at 37°C against 5 mM TES buffer, pH 7.0; the outside buffer was changed every 8 h. During this step, the laurate surfactant was removed and replaced by a phospholipid bilayer envelope. Then, the mixture was fractionated in a high-gradient magnetic field, generated by putting a tube of 0.078-inch inner diameter and about 10 cm in length, packed with magnetizable stainless steel wool, between the two poles of an electromagnet (Bruker BE-15, Karlsruhe, Germany), operating in a 1.5 T field. By pumping the mixture through this device, the excess vesicles flowed through while the MLs were captured on the steel wool. After switching off the magnetic field, the MLs were released from the filter device by a buffer stream at a high rate ($0.5\,L\,h^{-1}$) and collected. The ML preparations were stored at room temperature. Iron and phosphate were measured spectrophotometrically on a UVIKON 933 double beam UV/Vis spectrophotometer (Kontron Instruments, Milan, Italy) as described in [22]. As we observed earlier [22], the phosphate/iron ratio is indicative for the quality of the formed MLs. Theoretically, the mmol phospholipid/g Fe_3O_4 ratio equals 0.73 in case a 14 nm diameter iron oxide core is covered by a single bilayer, made up of 'ordinary' phospholipids. In practice, however, due to some variation among ML core sizes, this value can fluctuate between 0.60 and 0.85 for perfect bilayers. Lower values are suggestive for the presence of an incomplete bilayer, while higher values signify either deposition of multilayers or adherence of entire vesicles to ML phospholipids.

2.2.3 Transmission electron microscopy. TEM investigation of MLs was done by putting a drop of the sample onto a copper mesh coated with a Formvar film. Excess fluid was removed, and the sample was then stained with 2% uranylacetate solution. After drying, the specimen was viewed in a Zeiss EM 10°C transmission electron microscope to verify the presence of a phospholipid envelope surrounding the iron oxide core (see section 3).

3. Results

3.1 *Gadolinium(III)–Arsenazo binding*

Gd(III) forms a blue-green-coloured complex with Arsenazo. At pH 7.0 (5 mM TES buffer), the UV-Vis spectra in the range of 200–900 nm (UVIKON 933 apparatus) of a solution containing Arsenazo(III) dye (final concentration 0.04 mM) in the presence of increasing amounts of Gd(III) are shown in figure 2. The maximal absorption change occurs at 653 nm, which is a few nanometres lower than the value (658 nm) reported by Hvattum *et al*. [24]. Surprisingly, at a Gd(III)/Arsenazo ratio >1.0, this absorbance difference diminishes; the data points can be fitted well by a third-order polynomial function (figure 3). In case the total Gd(III) concentration exceeds 200 μM (in the actual

setup corresponding to a Gd(III)/Arsenazo molar ratio of 3.3), a precipitate is formed after 30 min of incubation. To avoid complications in Gd determinations due to both the third-order polynomial dependency of the absorption values at 653 nm ($A^{653\,nm}$) on the Gd(III) concentration, and the above-mentioned precipitation problems,

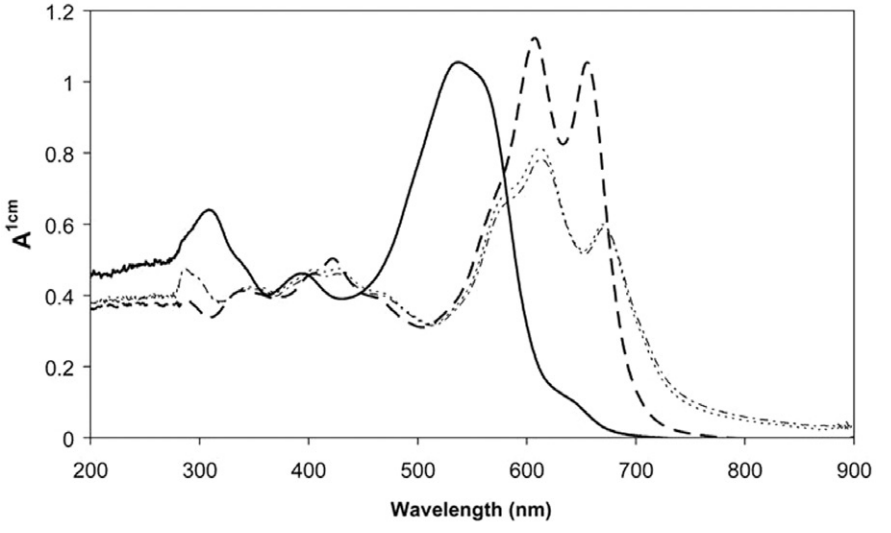

Figure 2. UV-Vis absorption spectra between 200 and 900 nm of Arsenazo (final concentration: 0.04 mM) in the presence of increasing amounts of Gd(III). The Gd(III)/Arsenazo ratios (mol mol^{-1}) equal 0 (solid line), 0.825 (dotted line), 1.675 (dashed line), and 2.5 (dashed-dotted line).

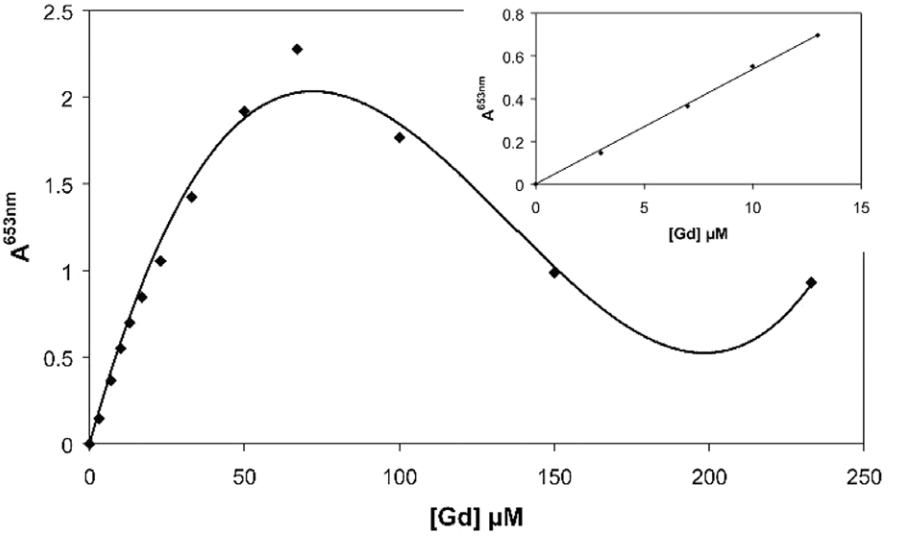

Figure 3. Changes in the absorbencies at 653 nm of Arsenazo (final concentration: 0.05 mM) in the presence of increasing amounts of Gd(III) at pH 7.0 (5mM TES buffer). The full line represents the best fitting polynomial as calculated by the Microsoft Excel® computer program. Inset: fitting of the first data points (<15 µM Gd(III) concentration) by linear regression.

we carefully performed (free) Gd(III) dosages in the detection window between 0 and 15 μM. In this range, the data points, indeed, can be fitted well by linear regression analysis ($r^2 = 0.998$), indicating a clear linear relationship between the absorbance measured at 653 nm and the concentration of free Gd(III) ions at low concentrations ($\leq$13 μM) using the Arsenazo III spectrophotometric assay (figure 3 inset). In this way, measurements of the absorptions at 653 nm can be directly and safely converted to concentrations of free Gd(III) ions. Starting from these values and taking into account the *total* Gd(III) concentration in the mixtures, the amount of immobilized Gd(III) can be calculated, allowing us to assess the average number of Gd(III) ions per vesicle or ML particle.

3.2 *Binding of gadolinium(III) to DTPA*

Next, the binding features of Gd(III), first confronted with DTPA and then mixed with Arsenazo, were checked. In practice, increasing amounts of Gd(III) (0.3 mL of solutions varying in concentration from 0 to 5 mM) were mixed with 0.684 mL of a 1 mM DTPA solution; subsequently, 0.3 mL of Arsenazo (5.5 mM) was added. In each tube, the final volume was adjusted to 3.3 mL with buffer. The $A^{653\,nm}$ values, obtained after a sixfold dilution of the samples with buffer, are shown in figure 4 (◆). The curve can be divided into two zones: in the lower Gd(III)/DTPA zone, only the background absorption of Arsenazo is observed, whereas at higher Gd(III) amounts, the $A^{653\,nm}$ values gradually increase as the (free) Gd(III) concentration increases. Each of the two sets of data can be fitted by straight lines which intersect at a Gd(III)/DTPA ratio of 0.96, indicating that the affinity of Gd(III) for DTPA is significantly higher than for Arsenazo.

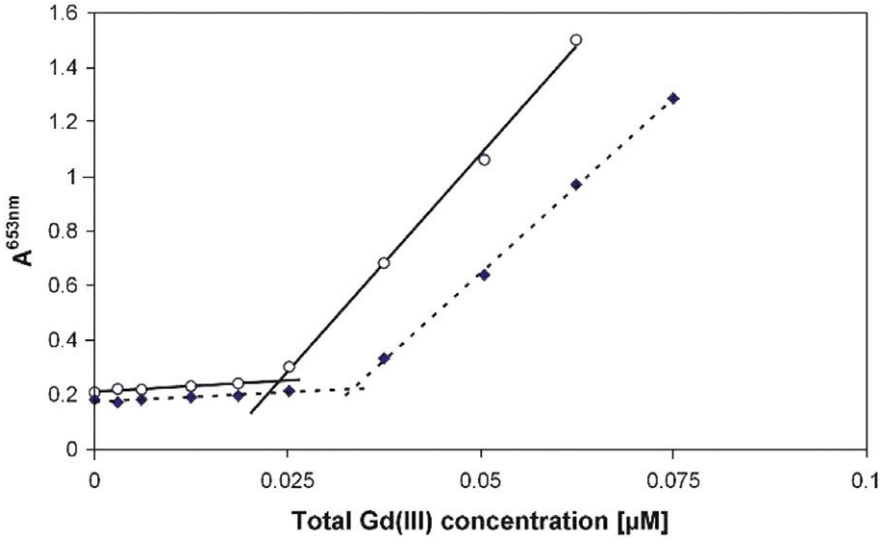

Figure 4. Changes in $A^{653\,nm}$ values of mixtures consisting of DTPA, Gd(III), and Arsenazo. The final concentration of DTPA, either pure (◆) or coupled to DMPE (○), and Arsenazo was 34.5 and 83.3 μM, respectively; the total concentration of Gd(III), as shown in the *x*-axis, varies from 0 to 75.75 μM. The measurements are done at pH 7.0 (5 mM TES buffer) after a sixfold dilution of the sample with buffer.

3.3 *Binding of Gadolinium to PE–DTPA containing vesicles*

The purpose of this experiment is to determine whether the strong DTPA–Gd(III) binding remains in cases when DTPA is derivatized with PE. Small unilamellar vesicles were first prepared (see section 2) by sonicating 6.84 μmol of DMPE–DTPA and 61.56 μmol of DMPC (the latter is included as matrix lipid) in 27 mL of 5 mM TES buffer. This vesicle stock solution was divided into 2.7 mL fractions. Following the modus operandi described in the previous section, each tube (amount of DMPE–DTPA = 0.684 μmol) was treated with 0.3 mL of one of the gadolinium solutions (see above) and then 0.3 mL of the Arsenazo stock solution (5.5 mM). As shown in figure 4 (○), two sets of $A^{653\,nm}$ values were again noticed, but in this case the break in the profile occurred at a Gd(III)/PE–DTPA ratio of 0.68, which is about a third lower than was noticed for non-derivatized DTPA. This result indicates that incorporation of the DMPE–DTPA adduct into small unilamellar vesicles leads to a reduction in the number of DMPE–DTPA conjugates available for complexation with free Gd(III) ions. This finding is in accordance with previous observations indicating that in small unilamellar vesicles, the outer phospholipid layer contains about two-thirds of the total phospholipid amount, while the inner layer is made up of about a third of the original amount [25]. Thus, it can be assumed that DMPE–DTPA adducts built into the inner layer are inaccessible to the highly polar, free Gd(III) ions, explaining the one-third difference we found here.

3.4 *Binding of Gd(III) to PE–DTPA containing MLs*

We also verified whether it is possible to incorporate the DMPE–DTPA adduct in the phospholipid bilayer coat of MLs. Following the protocol described in section 2, this was done by first preparing a stock solution of intramembraneously mixed DMPC–DMPG (9/1 molar ratio) MLs. The negatively charged phospholipid DMPG was included because, for electrostatic reasons, this considerably improves the colloidal stability of the MLs. The ML solution (1.5 mL) was then incubated for 4 h at 25°C with 1.5 mL of vesicles containing equimolar amounts of DMPC and DMPE–DTPA. The total lipid concentration of each of the starting ML and vesicle populations was 4.33 μmol mL^{-1}. After 4 h, the mixture was subjected to a high-gradient magnetophoresis cycle, i.e. four fractions of 0.75 mL each were pumped through the magnetic filter device and washed with 0.375 mL of buffer. After disconnecting the magnetic field, the magnetic particles were eluted from the stainless steel fibres with 3 mL buffer and collected. The ML fraction obtained in this way had an overall phospholipid content of 4.33 μmol mL^{-1}, and the phospholipid-to-magnetite ratio was 0.58 mmol g^{-1}. In transmission electron microscopy, the typical architecture, observed earlier for other ML types [22], is visible; i.e. the particles are spherical with an inner electron dense magnetite core with a diameter of about 15 nm, surrounded by an electron translucent layer corresponding to the hydrophobic part of the surrounding phospholipid bilayer (figure 5).

To determine whether or not the DMPE–DTPA adducts, originally present in the vesicle population at a concentration of 2.16 μmol mL^{-1}, have been percolated into the ML bilayer, the MLs were titrated with Gd(III) ions. In different test tubes, each containing 0.2 mL of the ML solution (0.87 μmol of phospholipid), increasing volumes (from 0 to 1.2 mL) of a 1 mM Gd(III) stock solution were added, followed by the

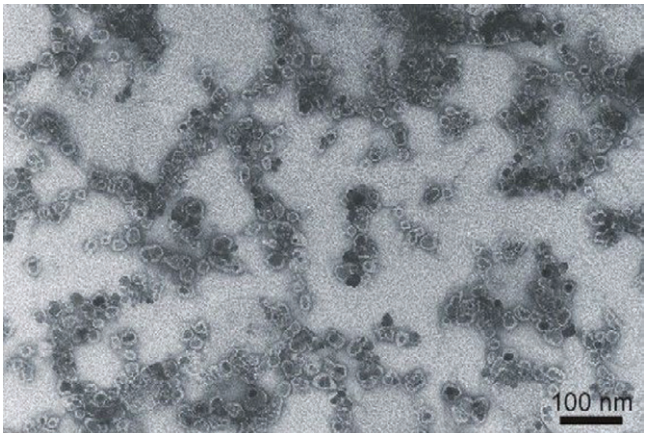

Figure 5. TEM images of MLs covered with Gd(III) ions. The particles contain an electron-dense subdomain magnetite crystal, on average 14 nm in diameter. The bright layer surrounding each core corresponds to the enveloping phospholipid bilayer. Bare scale: 100 nm.

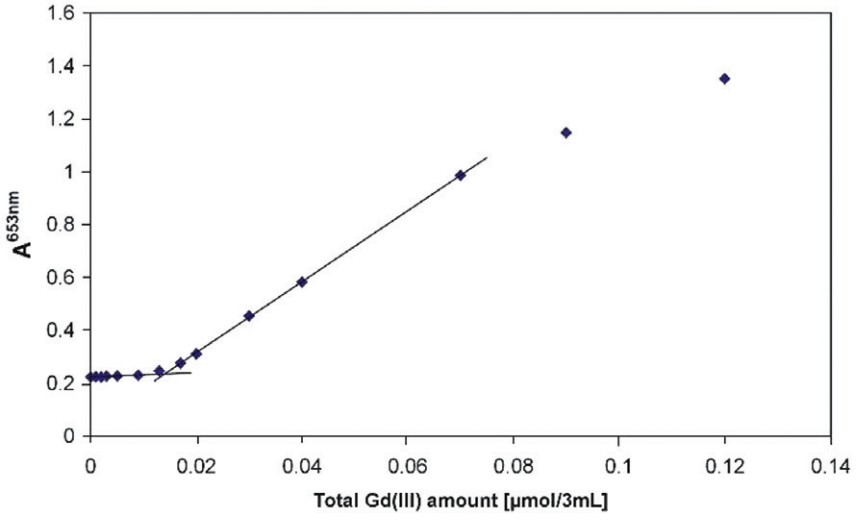

Figure 6. Gd(III) binding to DMPE–DTPA loaded MLs, measured with the Arsenazo dye at 653 nm. After a tenfold dilution of the incubation mixtures (see text), each sample (3 mL) contained 0.087 µmol of phospholipid and 0.15 µmol of Arsenazo; the Gd(III) content ranged from 0 to 0.12 µmol.

addition of 1 mL of a 1.5 mM Arsenazo indicator solution after 30 min. Finally, the volume was adjusted to 3 mL with TES buffer. Before measuring the $A^{653\,nm}$ values, the solutions were diluted 10 times with TES buffer. From figure 6, it appears that up to a Gd(III) concentration of about 0.015 µmol/3 mL, the absorption values correspond to the background absorption of pure Arsenazo, indicating that the added Gd(III) ions are captured by DMPE–DTPA present in the ML coat. At higher Gd(III) concentrations, the presence of free lanthanide ion is reflected by the increase in $A^{653\,nm}$. It is interesting

to note that the break in the curve is located at a point where 0.015 μmol of Gd(III) has been added to the mixture, which also contains 0.087 μmol of ML phospholipids. As will be discussed below, this means that approximately 17% of the ML lipids are DMPE–DTPA, clearly indicating that the DMPE–DTPA adduct did not merely percolate into the ML bilayer but was instead efficiently and stably incorporated.

4. Discussion

Gouin *et al.* [26] reported an affinity constant of $10^{-15.85}\,M^{-1}$ and $10^{-23.02}\,M^{-1}$ for Gd(III) binding to Arsenazo and DTPA, respectively. In our experimental setups (see figure 4), we found that this difference in affinity is large enough to reliably quantify unbound gadolinium. Although measurement of the absolute value of the Arsenazo–Gd(III) affinity constant(s) was not the purpose of this work, we tentatively suggest that the third-order polynomial dependency of gadolinium chelating to Arsenazo at Gd(III)/Arsenazo molar ratios >1 is caused by the binding of more than one Gd(III) ion to each Arsenazo molecule as the lanthanide ion concentration increases.

As compared with the study of Gd(III) binding to the water-soluble DTPA, the experimental conditions for unravelling the binding feature of the lanthanide ion to the DMPE–DTPA conjugate are more complex, since the conjugate is no longer water-soluble. Phospholipid vesicles, however, are unique structures to 'solubilize' amphiphilic molecules. To construct these colloidal structures, we purposely used dimyristoylphospholipids (DMPC and DMPG), because these structures are above their so-called gel-to-liquid crystalline phase transition temperature at room temperature, thereby creating a rather loose fatty acyl chain packing which favours the uptake of amphiphilic molecules. Also, the myristoyl fatty acyl chain residues are identical to those of the DMPE–DTPA conjugate, thereby minimizing the risk of inducing packing defects in the membrane structure. Figure 4 clearly shows that, in spite of the fact that the DTPA content (either in free form or linked to DMPE) is identical in both setups, the vesicle construct binds only two-thirds of the amount of Gd(III) chelated by free DTPA. This discrepancy can be explained by assuming that small sonicated vesicles with a diameter of 25–30 nm retain about one-third of the phospholipids (including DMPE–DTPA) in the inner leaflet and two-thirds in the outer one [26]. Most likely, the inner leaflet DMPE–DTPA will remain completely deprived of Gd(III), since it is well known that polar substances, including Gd(III), are not able to cross the hydrophobic interior of the membrane, and, moreover, for the same reason, the inside DMPE–DTPA molecules cannot flip-flop over the membrane. Therefore, we believe that steric hindrance is responsible for the lower extent of Gd(III) binding.

In spite of the fact that PE–DTPA is a powerful chelating agent that readily assembles into the walls of liposomes, one can argue that in the conjugate, the affinity of Gd(III) for DTPA is lowered, since one of the coordinating carboxylate groups of PE–DTPA has been sacrificed for coupling to the PE's amino group. This reasoning has also been raised by Lauffer *et al.* [8], Desreux *et al.* [27], Gaughan [28] and Sherry *et al.* [29], who suggest, in qualitative terms, that attachment of proteins or apolar chains to the DTPA chelate should (slightly) decrease its affinity for the lanthanide ion. Anyhow, this presumed lower stability will not seriously hamper the affinity constant,

since Arsenazo ($K_{ass} = 10^{-15.85}\,M^{-1}$; see above) remains unable to withdraw the ion from the complex.

The overall mechanism by which MLs are generated has been unravelled in one of our previous papers ([26] and references cited therein), and most probably also applies in the present setups. Briefly, it is shown that the lipid molecules first jump out of the donor membranes into the aqueous phase in a rate-limiting process. They then travel through the water and finally are taken up by the ML coat. The parameters which regulate this so-called aqueous transfer process are the medium (e.g. salt concentration, temperature, pH), the membrane features of both donors and acceptors (charge, curvature, physical state) and the transferring molecules themselves (quality of the polar headgroups and fatty acyl moieties) [26, 30, 31]. In the present work, we carefully selected experimental conditions to achieve a rapid distribution equilibrium. First, by choosing myristoyl chains, which are one of the shortest acyl chains encountered in biological membranes, a 'fluid' membrane (as opposed to a solid membrane) is produced at room temperature, which facilitates the escape of the conjugate from the donor vesicles. Second, by working in a low-ionic-strength medium (5 mM TES buffer), electrostatic repulsion forces between negatively charged DMPE–DTPA molecules at the membrane surface are promoted, thereby favouring their escape from the donor membrane [30, 31]. Third, by starting from highly curved vesicles (diameter of only 25–30 nm) in which a stressed phospholipid packing allows partial water penetration into part of the membrane structure, the free-energy barrier which kinetically regulates the rate-limiting escape step will be drastically reduced [32–34].

Based on this knowledge of phospholipid and membrane biophysics, we could successfully construct DMPE–DTPA containing MLs. The latter were prepared from DMPC/DMPG (90/10) MLs and DMPE–DTPA/DMPC (50/50) vesicles incubated in equimolar amounts with respect to phospholipid content. At the end, the amount of DMPE–DTPA detected in the ML acceptors was found to be about 17%, which corresponds to one-third of the quantity, originally present in the donor vesicles (50%). This observation can be rationalized by assuming, as mentioned above, that only the outer leaflet DMPE–DTPA molecules (which constitute two-thirds of the total amount, i.e. two-thirds of 50%) present in the donor vesicles are able to participate in the transfer process. In figure 7, a short outline is given of the partition of DMPE–DTPA over vesicle donors and ML acceptors. Presently, we have embarked on a study to further fine-tune the PE–DTPA content in the ML coat. We intend to realize this by enhancing the conjugate's concentration in the donor vesicles and/or by increasing the donor vesicle concentration with respect to that of the ML acceptors.

5. Concluding remarks

The main purpose of this work is the development of a biocompatible structure that can be used as a new type of MRI contrast agent. Indeed, in addition to the concentration of a few hundred Gd(III) ions on top of a liposomal structure which should improve the longitudinal relaxation of proton spins (the so-called T_1-effect), the ultrasmall iron oxide core will also create, very locally, magnetic field inhomogenities, thereby influencing the transversal relaxation (the so-called T_2^*-effect). Using optimal experimental conditions (Gd(III) payload, size of the magnetite grains, dose, applied

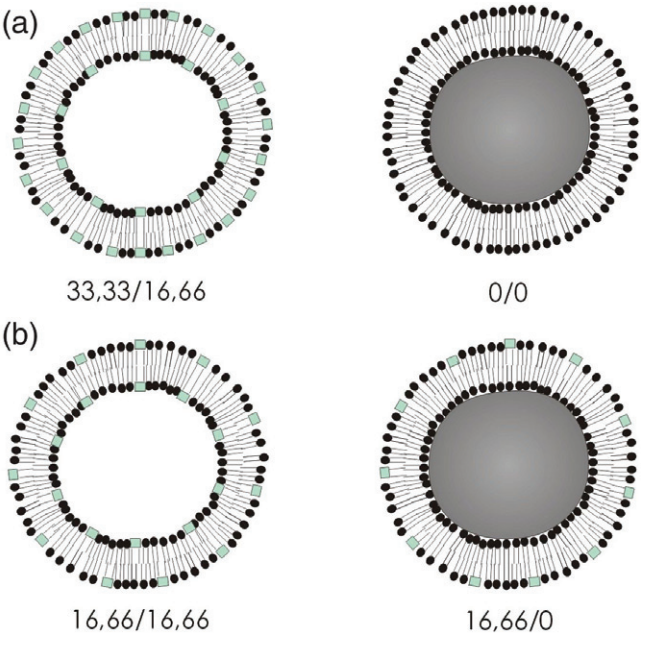

Figure 7. Schematic representation of the transfer movement of DMPE–DTPA from the DMPC/DMPE–DTPA (50/50) donor vesicles to the ML acceptors, composed of DMPC and DMPG. The open-circle phospholipids represent the matrix lipids DMPC and DMPG; the solid square represents the DMPE–DTPA. The situation at time = 0 (a) and at equilibrium (b) is shown. The numerator/denominator ratios refer to the distribution of DMPE–DTPA over outer and inner layer of vesicles and MLs (expressed as a percentage of the total amount of phospholipids present in vesicles and MLs).

pulse sequences, etc. [7, 18, 35]), the signals produced by this dual-enhancing relaxation particulate can be exploited to further improve the contrast in MRI pictures.

For *in vitro* synthesis of these bimodal contrast agents, we found that the colorimetric dye Arsenazo can be easily used to determine the complexation efficiencies of DTPA or DMPE–DTPA adducts for Gd(III) ions. The difference in affinity of Arsenazo or DTPA (-adducts) for Gd(III) ions is large enough to reliably quantify unbound gadolinium, thus allowing us to determine the average amount of gadolinium bound per ML.

In view of *in vivo* applications, the issue of mitigating the chemotoxicity of the Gd-MLs has to be further investigated. In biological fluids and tissues, the release of Gd(III) from the complex may be triggered by Zn^{2+}, Cu^{2+}, and/or Ca^{2+} transmetallation [36]. Thus, thermodynamic equilibrium constants, useful for evaluating *in vitro* stabilities of Gd(III)-chelates, are not infallible predictors of *in vivo* stability, and, possibly, subtle changes in formulations may be necessary to further improve the kinetic stability of the Gd complexes. Furthermore, the 20–30 nm particles developed in this work are too large to be cleared via the renal pathway. Rather, they end up mainly in the lymph nodes and bone marrow, and/or are taken up by the macrophages of the spleen or the liver where they can effectively block Kuppfer cell activity [3, 37, 38]. With respect to the further processing of the particles, however, the observations of Dupas *et al.* [39] and Schwendener *et al.* [40] are worth mentioning. These authors observed

that particles with a diameter similar to that of our MLs are secreted via the hepatobiliary route. It is highly likely that this pathway will be followed by the ML biocolloids, too, thereby drastically reducing the risk of toxic effects.

Acknowledgement

Supported by SBO project no. IWT/030238 to MDC. SJHS is the recipient of a research grant from the Institute for the Promotion of Innovation through Science and Technology in Flanders (IWT-Vlaandenen).

References

[1] A.M. Derfus, W.C.W. Chan, S.N. Bathia. *NanoLetters*, **4**, 11 (2004).
[2] C. Lizon, P. Fritsch. *Int. J. Radiat. Biol.*, **75**, 11 (1999).
[3] F. Roerdink, J. Dijkstra, G. Hartman, B. Bolscher, G. Scherphof. *Biochim. Biophys. Acta*, **677**, 79 (1981).
[4] A. Spencer, S. Wilson, E. Harpur. *Hum. Exp. Toxicol.*, **17**, 633 (1998).
[5] G.J. Stanisz, J.G. Li, G.A. Wright, R.M. Henkelman. *Magn. Reson. Med.*, **39**, 223 (1998).
[6] W. Krause (Ed.) *Contrast Agents I. Magnetic Resonance Imaging*, Topics in Current Chemistry No. 221, Springer, Berlin (2002).
[7] G.M. Lanza, P.M. Winter, S.D. Caruthers, A.M. Marowski, A.H. Schmieder, K.C. Crowder, S.A. Wickline. *J. Nucl. Cardiol.*, **11**, 733 (2004).
[8] R.B. Lauffer, T.J. Brady, R.D. Brown III, C. Baglin, S.H. Koenig. *Magn. Reson. Med.*, **3**, 541 (1986).
[9] D.G. Mitchell. *MRI Principles*, W.B. Saunders Co., Philadelphia, PA (1999).
[10] D. Weishaupt, V.D. Köchli, B. Marincek. *How does MRI wotk? An Introduction to the Physics and Function of Magnetic Resonance Imaging*, Springer, Heidelberg (2003).
[11] H. Gries. In *Contrast Agents I. Magnetic Resonance Imaging*, W. Krause (Ed.), pp. 1–24, Springer, Berlin (2002).
[12] R.B. Lauffer. *Chem. Rev.*, **87**, 901 (1987).
[13] S. Karlik, E. Florio, C.W. Grant. *Magn. Reson. Med.*, **19**, 56 (1991).
[14] A. Accardo, D. Tesauro, P. Roscigno, E. Gianolio, L. Paduano, G. D'Errico, C. Pedone, G. Morelli. *J. Am. Chem. Soc.*, **126**, 3097 (2004).
[15] P.L. Anelli, L. Lattuada, V. Lorusso, M. Schneider, H. Tournier, F. Uggeri. *Magn. Reson. Mater. Phys. Biol. Med.*, **12**, 114 (2001).
[16] G. Mangiapia, A. Accardo, F. Lo Celso, D. Tesauro, G. Morelli, A. Radulescu, L. Paduano. *J. Phys. Chem. B*, **108**, 17611 (2004).
[17] R. Rebizak, M. Schaefer, E. Dellacherie. *Bioconj. Chem.*, **9**, 94 (1998).
[18] H.-J. Weinmann, W. Ebert, B. Misselwitz, H. Schmitt-Willich. *Eur. J. Radiol.*, **46**, 33 (2003).
[19] V.P. Torchilin, V. Weissig, F.J. Martin, T.D. Heath, R.R.C. New. In *Liposomes—A Practical Approach*, V.P. Torchilin, V. Weissig (Eds), Chapter VII, 2nd Edn, pp. 193–229, Oxford University Press, Oxford (2003).
[20] F. Leclercq, M. Cohen-Ohana, N. Mignet, A. Sbarbati, J. Herscovici, D. Sherman, G. Byk. *Bioconj. Chem.*, **14**, 112 (2003).
[21] J.C. Dittmer, R.L. Lester. *J. Lipid Res.*, **5**, 126 (1964).
[22] M. De Cuyper, M. Joniau. *Eur. Biophys. J.*, **15**, 311 (1988).
[23] S.E. Khalafalla, G.W. Reimers. *IEEE Trans. Magn.*, **16**, 173 (1980).
[24] E. Hvattum, P.T. Norman, G.C. Jamieson, J.J. Lai, T. Skotland. *J. Pharm. Biomed. Anal.*, **13**, 927 (1995).
[25] M. De Cuyper, A. Crabbe, J. Cocquyt, P. Van der Meeren, F. Martins, M.H.A. Santana. *Phys. Chem. Chem. Phys.*, **6**, 1487 (2004).
[26] S. Gouin, F.M. Winnik. *Bioconj. Chem.*, **12**, 372 (2001).
[27] J.F. Desreux, J. Vincent, V. Humblet, M. Hermann, V. Comblin-Tholet, M.F. Tweedle. US Patent No. 6,056,939 (2000).
[28] G. Gaughan. In *Enhanced Magnetic Resonance Imaging*, V.M. Runge (Ed.), Chapter IX, pp. 105–136, Mosby, St. Louis, MO (1989).
[29] A.D. Sherry, W.P. Cacheris, K.-T. Khuan. *Magn. Reson. Med.*, **8**, 180 (1988).
[30] M. De Cuyper, M. Joniau, J.B.F.N. Engberts, E.J.R. Sudhölter. *Colloid. Surf.*, **10**, 313 (1984).

[31] M. De Cuyper, M. Joniau. *Biochim. Biophys. Acta*, **1027**, 172 (1990).
[32] M. De Cuyper, M. Joniau. *Progr. Colloid Polym. Sci.*, **84**, 456 (1991).
[33] D.L. Bernik, R.M. Negri. *J. Colloid Interf. Sci.*, **203**, 97 (1998).
[34] J.L. Harden, F.C. MacKintosh, P.D. Olmsted. *Phys. Rev. E.*, **72**, 011903 (2005).
[35] C. Chambon, O. Clément, A. le Blanche, E. Schouman-Claeys, G. Frija. *Magn. Reson. Imag.*, **11**, 509 (1993).
[36] W.P. Cacheris, S.C. Quay, S.M. Rocklage. *Magn. Reson. Imag.*, **8**, 467 (1990).
[37] J.W.M. Bulte, M. De Cuyper. *Meth. Enzymol.*, **373**, 175 (2003).
[38] V. Jacques, J.F. Desreux. In *Contrast Agents I. Magnetic Resonance Imaging*, W. Krause (Ed.), pp. 123–164, Springer, Berlin (2002).
[39] B. Dupas, G. Pradal, R.N. Muller, B. Bonnemain, K. Meflah, T. Bach-Gansmo. *Invest. Radiol.*, **36**, 509 (2001).
[40] R.A. Schwendener, R. Wüthrich, S. Duewell, E. Wehrli, G.K. von Schultheness. *Invest. Radiol.*, **25**, 922 (1990).